A Compact Quadrupole-Orbitrap Mass Spectrometer with FAIMS Interface Improves Proteome Coverage in Short LC Gradients

Authors

Dorte B. Bekker-Jensen, Ana Martínez-Val, Sophia Steigerwald, Patrick Rüther, Kyle L. Fort, Tabiwang N. Arrey, Alexander Harder, Alexander Makarov, and Jesper V. Olsen

Correspondence

jesper.olsen@cpr.ku.dk

Graphical Abstract

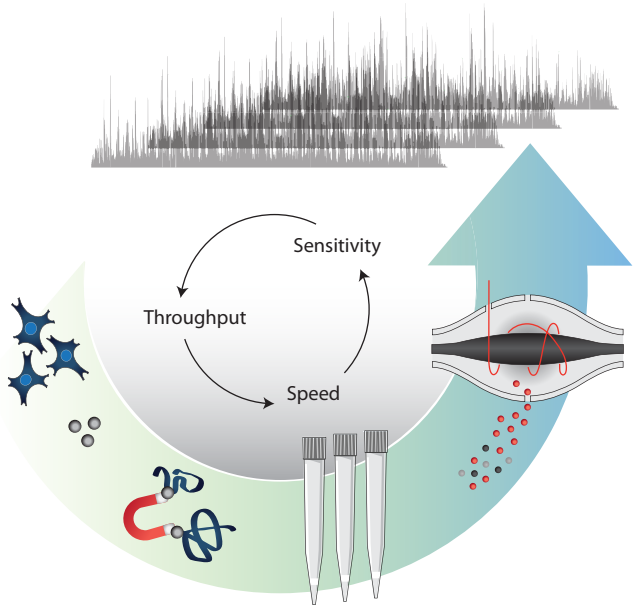

In Brief

Orbitrap Exploris 480 MS with FAIMS Pro provides fast, sensitive and robust profiling of proteomes when combined with Evosep One. The combination of Data Independent Acquisition (DIA) and FAIMS with single compensation voltages enables analysis of up to 2000 peptides per LC gradient minute and more than 5000 protein groups in twenty minutes. DIA-FAIMS based label-free quantitation achieves similar depth and quantitative accuracy as the well-established isobaric labelling approaches, but with less LC-MS measurement time, making it a good choice for large cohort of samples.

Highlights

- Increased proteome coverage with Orbitrap Exploris 480 MS and FAIMS using single compensation voltages and short LC gradients.
- Towards single-cell proteomics with high-sensitivity analysis of 5 ng HeLa with more than 1,000 proteins identified in 5 minutes using FAIMS and DIA.
- Deep proteome profiling across twelve rat organs tissues by label-free quantitation using DIA compared to TMT-multiplexing and turboTMT acquisition using phi-SDM.
- Rapid and sensitive phosphoproteomics with automated enrichment using Ti-IMAC magnetic beads and direct DIA analysis.

Bekker-Jensen et al., 2020, Molecular & Cellular Proteomics *19*, 716–729

https://doi.org/10.1074/mcp.TIR119.001906

⌘ *Author's Choice*

A Compact Quadrupole-Orbitrap Mass Spectrometer with FAIMS Interface Improves Proteome Coverage in Short LC Gradients*[S]

Dorte B. Bekker-Jensen‡**‖, Ana Martínez-Val‡‖, Sophia Steigerwald‡, Patrick Rüther‡, Kyle L. Fort§, Tabiwang N. Arrey§, Alexander Harder§, Alexander Makarov§, and Jesper V. Olsen‡¶

State-of-the-art proteomics-grade mass spectrometers can measure peptide precursors and their fragments with ppm mass accuracy at sequencing speeds of tens of peptides per second with attomolar sensitivity. Here we describe a compact and robust quadrupole-orbitrap mass spectrometer equipped with a front-end High Field Asymmetric Waveform Ion Mobility Spectrometry (FAIMS) Interface. The performance of the Orbitrap Exploris 480 mass spectrometer is evaluated in data-dependent acquisition (DDA) and data-independent acquisition (DIA) modes in combination with FAIMS. We demonstrate that different compensation voltages (CVs) for FAIMS are optimal for DDA and DIA, respectively. Combining DIA with FAIMS using single CVs, the instrument surpasses 2500 peptides identified per minute. This enables quantification of >5000 proteins with short online LC gradients delivered by the Evosep One LC system allowing acquisition of 60 samples per day. The raw sensitivity of the instrument is evaluated by analyzing 5 ng of a HeLa digest from which >1000 proteins were reproducibly identified with 5 min LC gradients using DIA-FAIMS. To demonstrate the versatility of the instrument, we recorded an organ-wide map of proteome expression across 12 rat tissues quantified by tandem mass tags and label-free quantification using DIA with FAIMS to a depth of >10,000 proteins. ***Molecular & Cellular Proteomics 19: 716–729, 2020. DOI: 10.1074/mcp.TIR119.001906.***

Deep proteome profiling of human cells can now be routinely achieved by shotgun proteomics using the latest advances in nanoflow liquid chromatography tandem mass spectrometry (LC-MS/MS) (1,2). However, comprehensive analysis of a human proteome typically requires days of mass spectrometric measurement time (3), making high-throughput analysis challenging and time-consuming. Therefore, new improved mass spectrometric technology and acquisition strategies are needed to overcome these limitations in current large-scale proteomics. The Orbitrap analyzer has become one of the major players in mass spectrometry-based proteomics (4). We have previously described the performance enhancement achieved over the different generations of the popular benchtop quadrupole-Orbitrap instruments, the Q Exactive™ series, for proteomics applications (5–7). The previous generation Q Exactive HF-X™ hybrid quadrupole-Orbitrap instrument incorporated a new peak-picking algorithm, a brighter ion source, and optimized ion transfers enabling productive HCD-MS/MS (8) acquisition above 40 Hz. These improvements collectively resulted in increased peptide and protein identification rates of up to fifty percent at short LC-MS gradients with more than 1000 unique peptides identified per minute (7). However, instrument performance after extended periods of continuous sample analyses could be comprised by contaminants entering the quadrupole and resulting in local charging and lower MS/MS sensitivity. This meant that regular preventative maintenance could be necessary to preserve high performance of the Q Exactive HF-X instrument. Moreover, the semi-stochastic nature of the data-dependent acquisition (DDA)[1]—the most popular tandem mass spectrometric acquisition strategy may create issues with reproducibility of peptide measurements between samples leading to the so-called missing value problem. To overcome the precursor selection problem inherent to DDA, data-independent acquisition (DIA) offers systematic measurement of all peptide ions regardless of their intensity by co-fragmenting all co-eluting peptides in broader precursor isolation windows. This provides wider dynamic range of the proteomes analyzed, improved reproducibility for identification and enabled better sensitivity and accuracy for quantification. The highly multiplexed fragment ion spectra in DIA require more elaborate processing algorithms for identification and quantification. These typically rely on spectral libraries previously recorded by data-dependent acquisition of similar sample types.

From the ‡The Novo Nordisk Foundation Center for Protein Research, University of Copenhagen, Copenhagen, Denmark; §Thermo Fisher Scientific, Bremen, Germany

Received December 11, 2019, and in revised form, February 3, 2020
Published, MCP Papers in Press, February 12, 2020, DOI 10.1074/mcp.TIR119.001906

The front-end high-field asymmetric waveform ion mobility spectrometry (FAIMS) (9–11) interface functions as an ion selection device and an electrospray filter that prevents neutrals from entering the orifice of the mass spectrometer while reducing chemical background noise. This "purification" of the electrosprayed ions typically results in improved robustness and sensitivity for proteomics experiments. The FAIMS Pro interface continuously selects and focuses ions at atmospheric pressure based on their differential mobilities in a high field *versus* a low electric field established by applying an asymmetric (*e.g.* bi-sinusoidal) voltage to at least one of the inner and outer electrodes. To prevent an ion species from being discharged, the FAIMS Pro interface applies a small DC potential, called the compensation voltage (CV), to the inner electrode to compensate for the ion drift resulting from the applied asymmetric waveform. Selection of an ion species is based on a combination of its gas-phase charge-state and collisional cross-section. CVs can be tuned such that only selected subsets of ions are transmitted through the electrodes thereby favoring multiply-charged peptide species and filtering out singly-charged chemical background ions. The CV is typically negative for positive ions and positive for negative ions. The advantage of FAIMS in the context of large-scale proteomics on the Tribrid™ Orbitrap systems (*i.e.* those incorporating a quadrupole mass filter and dual-pressure linear quadrupole ion trap in addition to the Orbitrap mass analyzer) has previously demonstrated to improve proteome coverage for single-shot proteomics with long gradients by CV sweeping (11) and reduce ratio compression in TMT experiment (12–14). However, potential advantages of FAIMS for short gradients using single CVs have not been explored. Likewise, FAIMS in combination with DIA has not yet been investigated. Here we describe a thorough performance evaluation of the hybrid quadrupole-Orbitrap Exploris 480™ MS in combination with short LC gradients using the Evosep One system. Standard DDA in combination with FAIMS identifies more proteins but fewer peptides resulting in a compromise between sequence coverage and proteome depth. This is not the case for DIA, where FAIMS results in identification of more proteins while maintaining the number of peptide identifications.

EXPERIMENTAL PROCEDURES

Cells—Human epithelial cervix carcinoma HeLa cells were cultured in DMEM (Gibco, Invitrogen), supplemented with 10% fetal bovine serum, 100U/ml penicillin (Invitrogen), 100 μg/ml streptomycin (Invitrogen), at 37 °C, in a humidified incubator with 5% CO_2.

Lysis—Cells were harvested at ~80% confluence by washing twice with PBS (Gibco, Life technologies) and subsequently adding boiling lysis buffer (5% sodium dodecyl sulfate (SDS), 5 mM tris(2-carboxyethyl)phosphine (TCEP), 10 mM chloroacetamide (CAA), 100 mM Tris, pH 8.5) directly to the plate. The cell lysate was collected by scraping the plate and boiled for an additional 10 min followed by micro tip probe sonication (Vibra-Cell VCX130, Sonics, Newtown, CT) for 2 min with pulses of 1 s on and 1 s off at 80% amplitude. Protein concentration was estimated by BCA.

Rat Tissue Preparation—The study was carried out following approved national regulations in Denmark and with an animal experimental license granted by the Animal Experiments Inspectorate, Ministry of Justice, Denmark. Three male Sprague-Dawley rats (Crl/S.D., male, 200 g, Charles River, Germany) were anesthetized with isoflurane. The animals were perfused (1.5 min, 30 ml/min) with isotonic saline containing protease inhibitors (0.120 mM EDTA, 14 μM aprotinin, 0.3 nM valine-pyrrolidide and Roche Complete Protease Inhibitor tablets (Roche), pH = 7.4). Tissues were quickly removed and snap frozen in isopentane on dry ice. Frozen organs were heat inactivated (Denator T1 Heat Stabilizor, Denator) and a portion of each tissue was transferred to an SDS solution (5% SDS, 25 mM Tris, pH 8.5) and homogenized by ceramic beads using steps of 20 s at 5500 rpm (Precellys 24, Bertin Technologies) until all tissue was clarified. The tissues were heated for 10 min at 95°C followed by micro tip sonication on ice and clarified by centrifugation (20 min, 16,000 × *g*, 4°C). Samples were reduced and alkylated by adding 5 mM tris(2-carboxyethyl)phosphine and 10 mM chloroacetamide for 20 min at room temperature.

Automated PAC Digestion—Protein digestion was automated on a KingFisher™ Flex robot (Thermo Fisher Scientific) in 96-well format. The 96-well comb is stored in plate #1, the sample in plate #2 in a final concentration of 70% acetonitrile and with magnetic Amine beads (ReSyn Biosciences) in a protein/bead ratio of 1:2. Washing solutions are in plates #3–5 (95% Acetonitrile (ACN)) and plates #6–7 (70% Ethanol). Plate #8 contains 300 μl digestion solution of 50 mM ammonium bicarbonate (ABC), LysC (Wako) in an enzyme/protein ratio of 1:500 (w/w) and trypsin (Sigma Aldrich) in an enzyme:protein ratio of 1:250. The protein aggregation was carried out in two steps of 1 min mixing at medium mixing speed, followed by a 10 min pause each. The sequential washes were performed in 2.5 min and slow speed, without releasing the beads from the magnet. The digestion was set to 12 h at 37 degrees with slow speed. The workflow is illustrated in supplemental Fig. S5*A*. Protease activity was quenched by acidification with trifluoroacetic acid (TFA) to a final concentration of 1%, and the resulting peptide mixture was concentrated on Sep-Pak (C18 Classic Cartridge, Waters, Milford, MA). Peptides were eluted with 2 ml 40% ACN, followed by 2 ml 60% ACN. The combined eluate was reduced by SpeedVac (Eppendorf, Germany) and the final peptide concentration was estimated by measuring absorbance at 280 nm on a NanoDrop 2000C spectrophotometer (Thermo Fisher Scientific). Peptides were preserved at −80 degrees for further analysis or loaded on EvoTips according to the manufacturer's protocol.

High-pH Fractionation—Peptides were fractionated using a reversed-phase Acquity CSH C18 1.7 μm 1 × 150 mm column (Waters, Milford, MA) on an UltiMate 3000 high-pressure liquid chromatography (HPLC) system (Thermo Fisher Scientific) operating at 30 μl/minute. Buffer A (5 mM ABC) and buffer B (100% ACN) were used. Peptides were separated by a linear gradient from 5% B to 35% B in 55 min followed by a linear increase to 70% B in 8 min. 46 fractions were collected without concatenation.

TMT Labeling—Rat peptides were TMT-labeled according to the overview in supplemental Fig. S4*A* with 10 μg of peptide and 4 μl of

[1] The abbreviations used are: DDA, data dependent acquisition; ACN, acetonitrile; APD, advanced peak detection; DIA, data independent acquisition; FAIMS, high-field asymmetric waveform ion mobility spectrometry; FA, formic acid; HCD, higher-energy collisional dissociation; HCTT, high capacity transfer tube; IT, maximum injection time; LC, liquid chromatography; *m/z*, mass-to-charge; MS, mass spectrometry; MS/MS, tandem mass spectrometry; PSMs, peptide spectrum matches; PTMs, post translational modifications; TFA, trifluoroacetic acid; TMT, tandem mass tags.

TMT reagent per channel. Labeling conditions were performed according to manufacturer's protocol. After labeling samples were pooled, acidified and concentrated on SepPaks (C18 Vac C18 Cartridge, 1cc/50 mg 55–105 μm Waters, Milford, MA). Peptides were eluted with 300 μl 40% ACN, followed by 300 μl 60% ACN and by 300 μl 80% ACN. The combined eluate was reduced by SpeedVac, resuspended in 5 mM ABC and offline high pH reversed phase fractionated as described above.

Automated Phosphopeptide Enrichment—Phosphopeptide enrichment was carried out on a KingFisher™ Flex robot (Thermo Fisher Scientific) in 96-well format as previously described (23,24) and also outlined in supplemental Fig. S5*B*. Two hundred micrograms of peptide were used for enrichments with 30 μl of magnetic Ti-IMAC HP beads (a prototype phosphopeptide enrichment product from ReSyn Biosciences), which is an improved version of the commercially available magnetic Ti-IMAC beads (ReSyn Biosciences). Briefly, the 96-well comb is stored in plate #1, 30 μl Ti-IMAC HP beads in 100% ACN in plate #2 and loading buffer (1 M glycolic acid, 80% ACN, 5% TFA) in plate #3. The sample volume is minimum doubled with loading buffer while kept in a total of 300 μl and added in plate #4. Plates 5–7 are filled with 500 μl washing solutions; loading buffer, 80% ACN, 5% TFA and 10% ACN, 0.2% TFA respectively. Plate #8 contains 200 μl 1% ammonia for elution. The beads were washed in loading buffer for 5 min at medium mixing speed, followed by binding of the phosphopeptides for 20 min and medium speed. The sequential washes were performed in 2 min and fast speed. Phosphopeptides were eluted in 10 min at medium mixing speed. The eluate is acidified with TFA and loaded directly on EvoTips.

Design of a Quadrupole Orbitrap Instrument—The Orbitrap Exploris 480 instrument (Thermo Fisher Scientific, Bremen, Germany) includes an atmospheric pressure ion source (API) interfaced to a radio-frequency ion funnel via a high-capacity transfer tube (HCTT), a quadrupole mass filter, a C-trap, an ion routing multipole (IRM), and an ultra-high field Orbitrap mass analyzer. Ions are formed at atmospheric pressure (in this work in a micro-electrospray ion source), pass through the HCTT to the ion funnel as described in Martins and coworkers (15) and then via a mass-selective injection flatapole as described in Scheltema *et al.* (16), into a bent flatapole. The S-shaped bent flatapole is implemented as two parallel printed circuit boards (PCB) with metal rods forming 4 mm gap between its rods, oriented in such a way that the line of sight from the HCTT is open for clusters and droplets to fly unimpeded out of the flatapole onto a dump. Ions are driven through the bent flatapole by an axial electric field created by a voltage divider on PCB stripes. After collisional cooling in the bent flatapole, ions are transmitted via a lens into a hyperbolic segmented-rod quadrupole. A known issue of quadrupole mass filter contamination has been addressed by introducing symmetrical ion loading. In this mode the DC polarity of quadrupole rods is regularly switched so that contamination becomes more symmetrical. After the quadrupole, ions are transferred to the C-trap via a short octapole and a split lens, now integrated with an independent charge detector. Ions fly through accelerating-only metal lenses of the C-trap into a nitrogen filled IRM and get trapped or fragmented there. The IRM pressure is measured directly by a Pirani gauge and varies in the range from 3 to 10 microbar. As in all other Orbitrap instruments of the Q Exactive (7,16,17) or Orbitrap Fusion™ series (18), fragmentation of ions in the IRM is achieved by adjusting the offset of the RF rods and the axial field to provide the required collision energy. Similarly, multiple precursor ions could be fragmented at their optimum collision energy without compromising the storage of preceding injections. Unlike previous instruments, the IRM is implemented using the same technology as the bent flatapole, *i.e.* using 4 shaped metal rods soldered to two PCBs separated by precision spacers. Also, a single RF supply drives the C-trap, transport multipole, and IRM at 3.1 MHz. During the return transfer to the C-trap, the same principle of electrodynamic squeezing is applied as in the Orbitrap analyzer. Specifically, IRM offset and C-trap lens voltages are slowly ramped up during the transfer so that ions face an increasing potential barrier as they approach lenses and therefore cannot get deposited on lens edges. Once ions are cooled inside the C-trap, voltages on all its electrodes are raised to the optimum for injection into the Orbitrap analyzer. Unlike all previous designs of C-trap, the pull-out pulse is applied only to the slotted electrode of the C-trap, which ensures strong ion focusing upon extraction so that losses on the edges of the slot are also reduced. Although reducing losses and contamination on the exit slit, such extraction requires additional focusing downstream of the C-trap with the help of an additional lens. The symmetrically suspended ultra-high field Orbitrap analyzer is open to pumping on both ends and combines better mechanical and electrical balancing with improved vacuum inside the trap, enabling higher resolution analyses with acquisition of longer transients. Ions are detected with 4 kV applied to the trap, which is somewhat lower than 5 kV in Q Exactive or Orbitrap Fusion series. Nevertheless, this still allows acquisition of transients at resolution settings ranging from 7500 to 480,000 at *m/z* 200 (16 and 1024 ms transients, respectively) in 7 steps differing by a factor of 2. The entire ion path from the ion funnel to Orbitrap analyzer is evacuated by a single, purpose-developed, 6-stage turbo pump PM902619A (Pfeiffer Vacuum, Asslar, Germany). UHV is realized without the use of knife-edge sealings by a "chamber-in-chamber" solution in which the pump also serves as a carrier for an inner chamber that houses the C-trap and Orbitrap analyzer. Pressure stages were matched to pumping ports by reducing the length of the hyperbolic-rod quadrupole mass filter, its pre-filters, and transport multipoles, without performance impairment. Ion funnel is evacuated by 120 m^3/h single-stage rotary vane pump (Sogevac® SV120 BI FC, Oerlikon Leybold Vacuum) and turbopump is backed by a dedicated Sogevac SV15 pump.

Processing of Transients—Transients detected in the Orbitrap mass analyzer are processed using an enhanced version of Fourier Transformation (eFT™) as described in Lange *et al.* (19). For TMT experiments, narrow m/z regions near TMT-10 reporter peaks (20,21) were processed by Phase-constrained signal deconvolution method (Phi-Transform) as described in Kelstrup *et al.* (22). This allowed use of special transient durations of 32 ms (resolution setting 15,000 at *m/z* 200) specifically for resolving isobaric TMT reporter ions in TMT 11-plex experiments.

FAIMS Pro—The new mass spectrometer shares several features with the latest Tribrid instruments such as the Orbitrap Fusion Lumos™ mass spectrometer and Orbitrap Eclipse™ Tribrid mass spectrometer. It has the same ion source, atmosphere-to-vacuum interface and user-facing software as the Orbitrap Fusion Lumos™ mass spectrometer. The shared design of the Orbitrap Exploris 480 mass spectrometer also enables it to be interfaced to the same front-end options that are available with the Tribrid instruments, such as the FAIMS Pro™ device and internal calibrant (EASY-IC™) source. Details of FAIMS Pro design and its characterization are presented in Pfammatter *et al.* (13). The unique feature of FAIMS Pro is the use of cylindrical electrodes that help to focus ions through the electrode assembly as they get carried by nitrogen carrier gas from front to back. With inner electrode blocking "line of sight" for clusters and dust particles, the additional benefit of interface protection from environmental effects is achieved. As this work uses higher flow rates than in previous nanospray experiments, method of FAIMS Pro operation includes an additional step of increased FAIMS carrier gas setting at the beginning of the LC gradient.

LC-MS/MS—All samples were analyzed on the Evosep One system using an in-house packed 15 cm, 150 μm i.d. capillary column with 1.9 μm Reprosil-Pur C18 beads (Dr. Maisch, Ammerbuch, Germany) using the pre-programmed gradients (60, 100, and 200 sam-

ples per day with flow rates of 1, 1.2 and 1.5 μl/min respectively). The column temperature was maintained at 60 °C using an integrated column oven (PRSO-V1, Sonation, Biberach, Germany) and interfaced online with the Orbitrap Exploris 480 MS. Spray voltage were set to 2 kV, funnel RF level at 40, and heated capillary temperature at 275 °C. For DDA experiments full MS resolutions were set to 60,000 at m/z 200 and full MS AGC target was 300% with an IT of 25 ms. Mass range was set to 350–1400. AGC target value for fragment spectra was set at 200% with a resolution of 15,000 and injection times of 22 ms and Top12. Intensity threshold was kept at 2E5. Isolation width was set at 1.3 m/z. Normalized collision energy was set at 30%. For DIA experiments full MS resolutions were set to 120,000 at m/z 200 and full MS AGC target was 300% with an IT of 45 ms. Mass range was set to 350–1400. AGC target value for fragment spectra was set at 1000%. 49 windows of 13.7 Da were used with an overlap of 1 Da. Resolution was set to 15,000 and IT to 22 ms. Normalized collision energy was set at 27%. All data were acquired in profile mode using positive polarity and peptide match was set to off, and isotope exclusion was on. Default settings were used for FAIMS with voltages applied as described in the manuscript, except gas flow, which was applied with 3 L/min in the first minute of the method and spray voltage which was set to 2.3 kV. For TMT experiments the turbo-TMT was enabled, MS/MS data was recorded in centroid mode. Isolation window was set to 0.7 Da and first mass was set to 100 *m/z*.

Rat Tissue Specific Library Generation—A pool from each tissue was generated using 40 μg of peptide from a given tissue from each independent rat. Each of the tissue pools were fractionated using high-pH reversed phase fractionated as described above into 46 fractions. For each tissue, the fractionated proteome was analyzed twice on the Evosep One with the column details described above and using the pre-programmed gradient (200 samples per day). Around 250 ng from each fraction was analyzed on a Q-Exactive HF-X using a MS/MS resolution of 15,000, injection time of 22 ms and a Top12 method. Another 250 ng was then analyzed on an Orbitrap Fusion Lumos with FAIMS using a MS/MS resolution of 30,000, injection time of 54 ms and a Top6 method and a CV of −45 V for FAIMS.

Raw Data Processing—All DDA raw files were processed with MaxQuant (25) v1.6.7.0 using the integrated Andromeda Search engine (26). All HeLa data is searched against a target/decoy version of the human Uniprot Reference Proteome without isoforms (21,074 entries), whereas all rat files are searched against the rat Uniprot Reference Proteomes with and without isoforms (21,662 entries + 9,900 entries for isoforms) and the mouse Uniprot Reference Proteome without isoforms (22,286 entries),all with January 2019 release. First search peptide tolerance was set to 20 ppm, main search peptide tolerance was set to 4.5 ppm. Fragment mass tolerance was set to 20 ppm. Trypsin was specified as enzyme, cleaving after all lysine and arginine residues and allowing up to two missed cleavages. Carbamidomethylation of cysteine was specified as fixed modification and protein N-terminal acetylation, oxidation of methionine, deamidation of asparagine and glutamine and pyro-glutamate formation from glutamine were considered variable modifications with a total of 2 variable modifications per peptide. “Maximum peptide mass” were set to 7500 Da, the “modified peptide minimum score” and “unmodified peptide minimum score” were set to 25 and everything else was set to the default values, including the false discovery rate limit of 1% on both the peptide and protein levels. The TMT proteomes were searched independently with further specification of TMT 11-plex as label with a reporter ion mass accuracy of 0.002 Da. For the rat proteomes, 12 different searches were performed independently with the “match between runs” feature enabled between fractions. All DIA raw files were processed with Spectronaut version 13 (Biognosys, Zurich, Switzerland). Project specific spectral libraries were imported from the separate MaxQuant analyzes of the combined analysis of the 2 × 46 pre-fractionated fractions of each tissue, and DIA files were analyzed using default settings disabling the PTM localization filter. Mass tolerance/accuracy for precursor and fragment identification was set to default settings. Up to 6 fragments were employed for library generation. FDR at peptide and protein level was set to 1% using a mutated decoy model (27). For matching of DIA data to spectral library, the applied mass and retention time tolerances (for both MS1 and MS2) are dynamic based on the *m/z* of the targeted ion and the retention time of the scan. The calibration is done for each run individually.

Phospho-enriched samples from rat tissues were processed in Spectronaut using a library-free approach (directDIA) including phosphorylation on STY as a variable modification, Rat database with isoforms and mouse database without isoforms were used for identification PTM localization cut-off was set to 0.75. Spectronaut v13 uses the localization algorithm as described in Bekker-Jensen *et al.* (28).

Data Analysis—DIA results from each independent tissue were merged by gene name. For quantification in DIA, we used standard settings in Spectronaut (v13) for quantification at MS2 level. Proteins, which were not quantified in all three replicates for at least one tissue were discarded for further analysis. Missing values were imputed in Perseus using values from a normal distribution (width = 0.3, downshift = 1.8). For quantification in TMT analysis, Reporter intensities from proteinGroups.txt table were used. TurboTMT data was filtered to remove proteins not quantified in all channels in three independent experiments. Intensities across channels were log2 transformed and normalized using quantile normalization. Batch effect between independent TMT experiments was removed using “ComBat” function implemented in the sva package (29) in R. For clustering, TMT and DIA data were separately transformed by z-score. For comparison with TMT, the average of duodenum, jejunum and ileum values for each independent rat was used. Finally, proteins were clustered using Euclidean distance in Perseus. Principal Component Analysis (PCA) was performed using proteins quantified in all experiments (either DIA or TMT), using the “prcomp” function in R. Phospho-DIA data was searched with directDIA in Spectronaut and the report output collapsed to either “modification-specific-peptide” or “phospho-site” tables using the Perseus plugin previously described(28). Phosphosite intensities were log2 transformed and missing values were imputed in Perseus using values from a normal distribution (width = 0.3, downshift = 1.8). Afterward, intensities were normalized using loess function implemented in the limma package in R, and ANOVA test was performed using an FDR < 1%. Phosphosite intensities were z-score transformed and clustered using Euclidean distance.

Experimental Design and Statistical Rationale—Number of replicates were denoted for all results where statistical analysis was performed and marked in the figures. Figure legends provided further clarification of statistical tests and criteria for determining significance in each case. For HeLa single-shot analysis, the same digest was frozen in aliquots and loaded on Evotips prior to analysis. Characterization of FAIMS CV settings were performed in duplicates for both DDA and DIA, whereas technical triplicates were performed for the remaining measurements at 60 samples per day and quadruplicate measurements for the 200 samples per day runs. Rat tissues were prepared from three independent rats and aliquots were frozen after PAC digestion. Phosphopeptide enrichment were performed separately from all samples.

RESULTS AND DISCUSSION

A Compact Quadrupole-Orbitrap Instrument for Proteomics—The Orbitrap Exploris 480 mass spectrometer combines a compact hybrid quadrupole-Orbitrap design with increased

performance in high-throughput analysis. Compared with the Q Exactive HF™ (16) and HF-X (7) mass spectrometers that use the same combination of analyzers, the entire layout of the instrument was reconfigured to enable a more compact and robust platform, which is easier to service. Furthermore, the bent flatapole, quadrupole, independent charge detector and ion routing multipole were all redesigned to address the enhanced requirements on the instrument. (Fig. 1*A*). However, the backbone of the new design is a new pumping concept, combined with a new layout of ion optics, C-trap electrodes, and Orbitrap electrodes. The requirement of ultra-high vacuum (UHV) in the 10E-10 or even 10E-11 mbar range for Orbitrap analysis of ions formed at atmospheric pressure has previously necessitated a bulky, multi pump vacuum system, which represented the major constraint on the overall design and size of the instrument. The main technical innovation realized in this new instrument concept is a single, purpose-developed, six-stage turbo pump that evacuates the entire path from the ion funnel to the Orbitrap analyzer. This enables a drastic reduction of instrument footprint and volume and enables easier access to all ion-optical components. Finally, several added front-end devices were enabled, *i.e.* FAIMS Pro interface and internal calibrant (EASY-IC) source, to extend the functionality of the instrument. Although atmosphere-to-vacuum interface and most ion-optical elements are quite similar in function and performance between the Q Exactive HF-X and the Orbitrap Exploris 480 MS instruments, a number of improvements were introduced to operation of the new mass spectrometer as described under Experimental Procedures.

Data-dependent Acquisition with FAIMS—To evaluate the performance of the instrument for proteomics we analyzed single-shot HeLa proteomes using short LC gradients both with and without FAIMS. HeLa cervix carcinoma cells were harvested in 5% SDS buffer and tryptic digests were prepared using an automated workflow by protein aggregation capture (PAC) (30) and proteolytic digestion with endoproteinase Lys-C and trypsin on magnetic beads using a KingFisher™ Flex robot (24). To minimize overhead time between LC-MS/MS runs and maintain robustness and reproducibility of LC separations over hundreds of injections, we made use of the Evosep One (31) system with short gradients in the range from 5 to 21 min enabling analysis of 60–200 samples per day. Although it utilizes a fundamentally different design, the Orbitrap Exploris 480 MS can achieve the same MS/MS scanning speed as the Q Exactive HF-X instrument when using the same transient and maximum injection times for optimal parallel mode of acquisition (7). All DDA experiments were therefore performed with a fast scanning top12 method encompassing a MS1 survey scan recorded at 60,000 resolution followed by twelve HCD scans with maximum allowed injection time of 22 ms and 15,000 resolution equivalent of 28 Hz MS/MS scan speed (Fig. 1*B*). To identify the optimal FAIMS settings for maximum proteome coverage we performed a systematic stepwise CV sweep from −80 V to −30 V with 5 V intervals and benchmarked the number of peptides and proteins identified at each CV setting with a standard DDA run

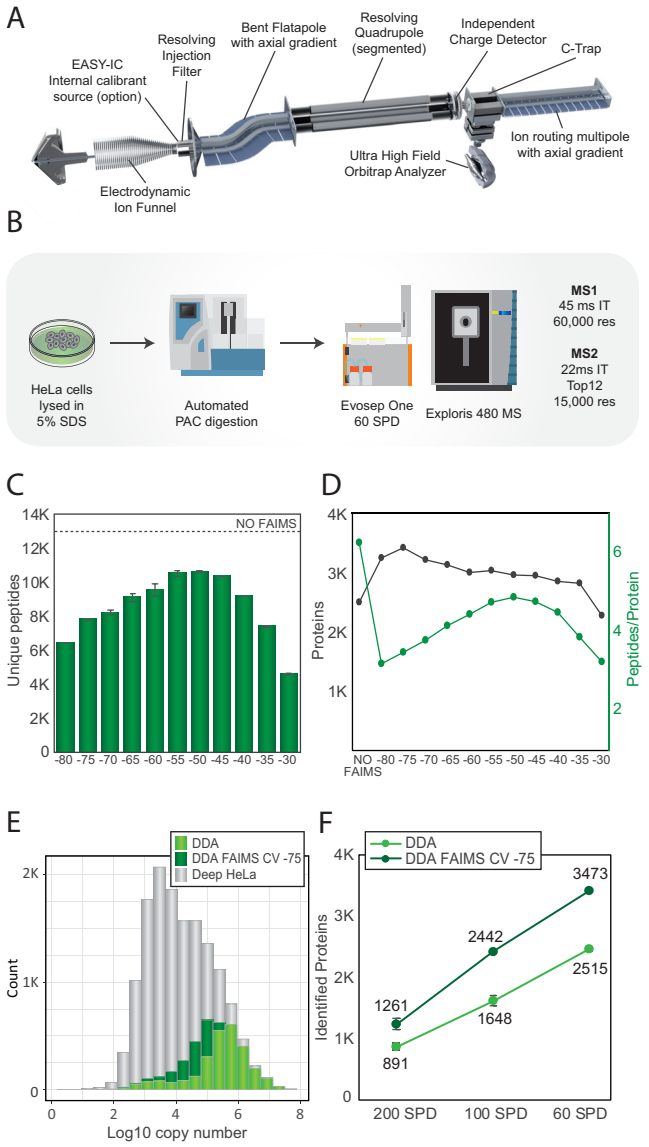

FIG. 1. ***A*, Hardware overview of the Orbitrap Exploris 480 MS instrument.** *B*, Experimental workflow for HeLa measurements. *C*, Barplot depicting the number of unique peptides identified using different compensation voltages with FAIMS. The number represented is the average of two replicates. Dashed line represents the average number of peptides identified in a DDA experiment without FAIMS. *D*, Average number of proteins in black with and without using FAIMS with different compensation voltages. In green, number of peptides identified per protein. The plotted values are the average of at least two technical replicates. *E*, Histogram of the protein abundance distribution represented as copy number in log10 scale of a deep HeLa proteome (gray) overlaid with 21 min single shot analyzes with FAIMS CV of −75 V (dark green) and without FAIMS (light green). *F*, Number of proteins identified from 500 ng of peptide using DDA (light green) or DDA with FAIMS and optimal CV of −75 V (dark green) in different gradient lengths: 200 SPD, 100 SPD and 60 SPD.

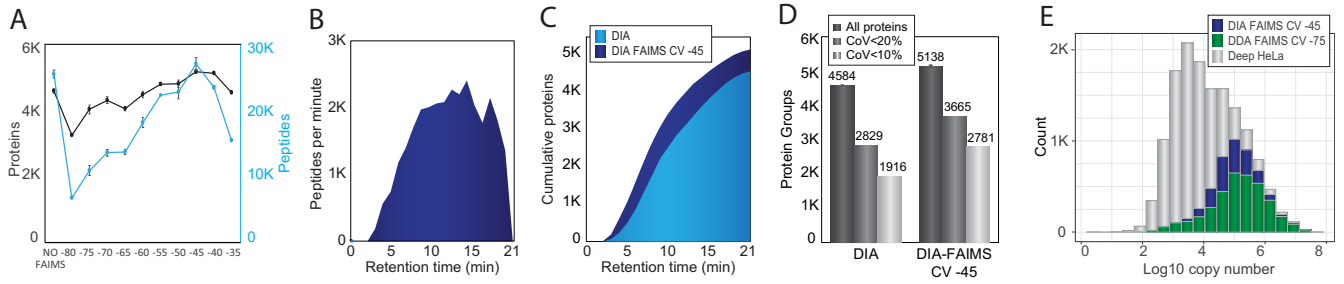

FIG. 2. ***A*, In black, number of proteins quantified from 500 ng of peptide in 21 min in a DIA experiment without FAIMS and with FAIMS using different compensation voltages.** In blue, number of peptides quantified in the same experiments. The plotted values are the average of at least two technical replicates. *B*, Visualization of peptide identification across the gradient length for DIA run with CV of −45 V with FAIMS and 500 ng load. *C*, Cumulative protein identifications across the gradient for DIA runs without (light blue) and with CV of −45 V with FAIMS (dark blue). *D*, Bar chart of all protein identifications (dark gray), proteins with coefficient of variation below 20% (gray) and below 10% (light gray) for DIA with and without CV of −45 V with FAIMS. *E*, Histogram of the protein abundance distribution represented as copy number in log10 scale of a deep HeLa proteome (gray), and in a single shot analysis of 21 min using DDA and optimal CV of −75 V with FAIMS (dark green) or using DIA and optimal CV of −45 V with FAIMS (blue).

without FAIMS. With 500 nanograms of HeLa peptides injected on column and analyzed with the 21 min (60 samples per day) gradient we observed a similar peptide distribution across the CV range as shown previously (11) with maximum peptide identification for CV of −50 V (Fig. 1*C* and supplemental Table S1). All DDA files were analyzed with MaxQuant (25) applying a one percent false discovery rate (FDR) at both peptide and protein level. The reproducibility and separation power of the FAIMS device judged by the replica runs suggests that a difference of more than 10 V between CVs is required to minimize overlaps (supplemental Fig. S1*A*). At a CV of −40 V and lower, singly-charged precursors were significantly reduced, whereas multi-charged precursors are spread across the CV range (supplemental Fig. S1*B*). None of the FAIMS files resulted in the same number of identifications as the run without FAIMS at 12,700 peptides. Conversely, all FAIMS runs except the one with a CV of −30 V achieved significantly higher number of protein identifications with a CV of −75 V providing the best coverage with 3473 proteins (representing 38% more than the 2515 proteins identified without FAIMS). However, the increased proteome depth with FAIMS comes at a cost of lower sequence coverage at single CVs (Fig. 1*D*). Surprisingly, a CV of −75 V provides the best protein coverage, but the smallest number of peptides resulting in only about three peptides per protein on average (Fig. 1*D* supplemental Table S1). At a CV of −75 V, we are operating at the edge of the peptide intensity distribution whereby a very small fraction of peptides is transmitted through the FAIMS device. The success of this CV setting is therefore highly dependent on the general performance of the instrument, as any loss in sensitivity will immediately result in a dramatic decrease in protein identification. It only works well when the total ion flux in MS/MS mode is high as measured by total ion current chromatogram (TIC) distributions plot (supplemental Fig. S1*C*). To assess the dynamic range of the proteins covered we overlapped the identifications with the deepest HeLa proteome to date with copy number estimates for 12,600 protein-coding genes (3). In the DDA-FAIMS experiments, we not only cover more proteins compared with the DDA without FAIMS, but we are also able to dig deeper into the HeLa protein abundance distribution covering significantly more of the dynamic range (Fig. 1*E*). The observed increase in the number of proteins identified with FAIMS operated with a CV of −75 V compared with runs without FAIMS is true for all gradients tested with even higher gains at shorter gradients, possibly because of concentration of the MS/MS signal intensity (Fig. 1*F*). We observed a 41% and 48% gain in number of proteins identified using gradients for 200 samples and 100 samples per day, respectively (Fig. 1*F*). Previously, it has been shown that in longer gradients switching CVs internally during the LC-MS/MS analysis improves peptide coverage[11]. However, with a current overhead time of 25 ms between individual single CVs, it is more suitable for gradients longer than the ones used in the current study.

Data-independent Acquisition with FAIMS—Next, we wanted to test if the benefits of applying FAIMS with a single CV could be extended to DIA. We again started by performing a CV sweep from −80 V to −35 V in steps of 5 V and compared the number of quantified peptides at each CV with an equivalent LC-MS/MS run without FAIMS. All DIA files were analyzed using the 60 samples per day gradient and processed with Spectronaut(23) software using a project-specific spectral library recorded at the same chromatography settings consisting of ~105,000 tryptic HeLa peptides and nearly 10,000 proteins for the analysis. We previously demonstrated that DIA provides higher proteome coverage than DDA with short gradients on a Q Exactive HF-X instrument (7). This is also the case with the Orbitrap Exploris 480 MS whereby we identified up to 4587 HeLa proteins in a single run using DIA, which corresponds to 35% more proteins than by DDA. Importantly, in contrast to the DDA-FAIMS analysis, we found that FAIMS-DIA worked best at a CV of −45 V with more identifications of peptides and 5138 proteins compared with a DIA run without FAIMS (Fig. 2*A* and supplemental Table

S2). Furthermore, DIA-FAIMS reaches impressive identification rates of up to 2500 peptides per minute of gradient time (Fig. 2*B*). This translates to a consistent gain in protein identifications across the gradient for DIA-FAIMS compared with classic DIA (Fig. 2*C*). These results highlight how the use of FAIMS in DIA mode not only increases proteome coverage, but also maintains the peptide identification rate in DIA mode without FAIMS. Even though FAIMS mobility separation results in a reduction in measured fragment ions, the increase in proteins identified is the result of more ions being sampled in MS/MS mode in DIA-FAIMS compared with DDA (supplemental Fig. S2*A*–S2*B*). In proteomics, it is not only central to identify as many peptides and proteins as possible but high quantitative precision is equally important. To test the impact of FAIMS on the quantitative accuracy, we analyzed the reproducibility of protein intensities between replicates. For DIA-FAIMS 71% of the 5,138 identified proteins were reproducibly quantified with a coefficient of variation below 20 and 54% with a coefficient of variation below 10% (Fig. 2*D*). In contrast, DIA analyzes without FAIMS decreased the number of consistently quantified proteins with a coefficient of variation below 20% to 2,829 representing only 60% of the total 4,584 proteins quantified (Fig. 2*D*). Importantly, this highlights that no compromise on quantitative accuracy is observed for the additional proteins identified with DIA-FAIMS. Compared with DDA-FAIMS, we observe that around 50% additional proteins identified in DIA-FAIMS match the same proteome abundance distribution range (Fig. 2*E*).

Sensitive Analysis with FAIMS and Very Short Gradients—Given the significant increase in protein identifications with 500 ng HeLa digest analyzed with FAIMS using the 60 samples per day gradient, we wondered whether this gain could also be achieved at decreased sample load. We analyzed 5 ng of tryptic peptides loaded on column equivalent to ~30–50 HeLa cells. For optimal sensitivity, the gradient was shortened to 5 min (200 samples per day) and samples were analyzed using both DDA and DIA with and without FAIMS. For such low amounts, it is required to enhance the MS/MS sensitivity by increasing the resolving power and injection times to 30,000 resolution and 54 ms, respectively. Moreover, we observed that a slightly shifted CV to −50 V is optimal (supplemental Fig. S3*A*). To maintain good quantitative accuracy it is required to reduce the cycle time from 2 s to 1 s (supplemental Fig. S3*B*). The very low amount is a challenge for standard DDA, where we only identify 26 proteins (Fig. 3*A*). With DDA-FAIMS, the identifications increased by a factor of 10 to 281 proteins (Fig. 3*A*). On the other hand, classic DIA further increased proteins identified to 547, whereas DIA-FAIMS is superior with more than 1,000 proteins identified (Fig. 3*A* supplemental Table S3). Additionally, FAIMS enhanced the reproducibility of DIA quantification, based on the number of proteins quantified with coefficient of variation below 20% (Fig. 3*B*). The observed 10-fold increase in number of proteins for the DDA-FAIMS compared with DDA without FAIMS suggests that DDA-FAIMS is ideally suited for DDA analysis of very low input material. The main reason for this is that FAIMS is capable of effectively removing the singly-charged background ions from ambient air and the electrospray buffer, which otherwise take up a lot of C-trap capacity when minute amounts of peptide mixtures are analyzed (Fig. 3*E*). This issue is best illustrated by the scaled total ion current chromatograms (TICs), where the background level in the DDA experiment is very high (Fig. 3*C*), whereas with DDA-FAIMS the background is very low and hence the peptide signals are significantly higher (Fig. 3*D*). This enhancement in the spectral quality by FAIMS is also striking when quantifying the number of ions measured in the full-scan MS1 spectrum during the gradient, where FAIMS has a much lower starting background level but 10-fold higher levels during peptide elution from 1.5 to 4 min (Fig. 3*F*).

Rat Tissue Specific Protein Atlas—The ability to quantify proteins and their post-translational modifications between cell states or cell types at a large scale is important for understanding protein regulation and dynamics in health and disease. The Orbitrap Exploris 480 mass spectrometer provides high sequencing speed and sensitivity and is therefore well suited for deep proteome profiling across many conditions. To identify the optimal quantitative proteomics workflow for large-scale proteome expression studies, we compared tandem mass tags (TMT11-plex) with DIA-based label-free quantification of 12 tissues covering the major mammalian organs from three individual male rats (Fig. 4*A*). To preserve the *in vivo* state of the organ proteomes and phosphoproteomes, the excised tissues were heat-inactivated[33] and homogenized in 5% SDS buffer. Extracted proteins were PAC precipitated on magnetic beads and digested with Lys-C and trypsin. All LC-MS/MS experiments were analyzed using the 21 min gradient (60 samples per day) on the Evosep One. For the DIA-based label-free quantification we analyzed each sample with the application of FAIMS to evaluate if it also provides benefits for complex organ proteome analyzes. Because spectral libraries are required for DIA, we performed deep proteome profiling by offline high-pH (HpH) reversed phase fractionation of the organ digests and analyzed each fraction by DDA analysis with and without FAIMS. Analyzing 46 HpH fractions from each of the 12 tissues ±FAIMS at CV of −45 V resulted in 1104 LC-MS/MS runs. Although each tissue required 32 h of LC-MS measurement time, all tissues collectively needed 18.4 days of total mass spectrometric measurement time. The peptide coverage in each tissue varied from 50,000 unique peptides identified in skeletal muscle to 100,000 identified in testis (Fig. 4*B*). The number of identified peptides generally correlates with the number of proteins identified in each organ with testis representing more than ten thousand proteins (Fig. 4*C*). Combining the DDA analyzes with and without FAIMS slightly improves the depth of the library on both peptide and protein level. The observed discrepancy in identifications likely reflects the dif-

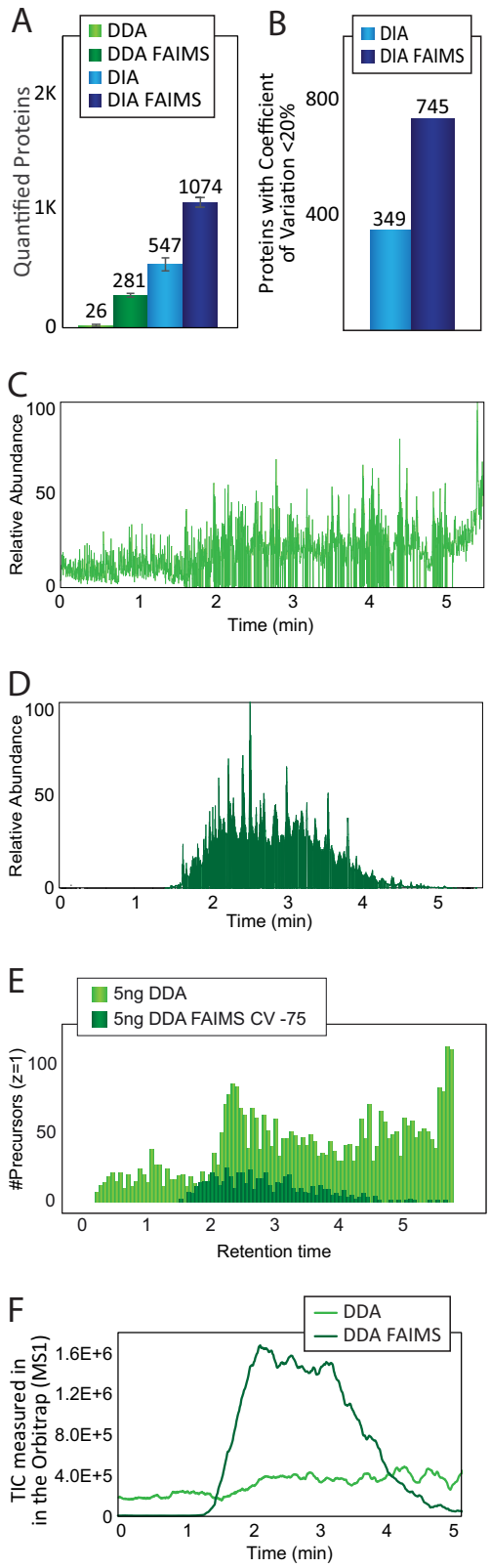

FIG. 3. ***A*, Bar chart showing the number of proteins identified in 5 min gradients (200 samples per day) using 5 ng load.** Light green bars correspond to DDA acquisition settings, dark green bars correspond to DDA with optimal CV with FAIMS, light blue bars correspond to DIA acquisition and dark blue bars correspond to DIA using FAIMS. Plotted values are the average between at least three replicates. *B*, Bar chart showing the number of proteins quantified with a coefficient of variation below 20% in DIA experiments with FAIMS (dark blue) or without FAIMS (light blue). *C*, Chromatogram of a DDA run from 5 ng using a 5 min gradient showing the relative abundance of the total ion current signal. *D*, Chromatogram of a DDA run with FAIMS (CV −75) from 5 ng using a 5 min gradient showing the relative abundance of the total ion current signal. *E*, Histogram showing the abundance distribution of precursors with charge +1 during a 5 min gradient using a sample loading of 5 ng in a DDA run (light green) or a DDA with FAIMS at CV −75 (dark green). *F*, Plot of the TIC measured in the Orbitrap analyzer in MS1 scans across time in a 5 min gradient using a sample loading of 5 ng in a DDA run (light green) or a DDA with FAIMS at CV-75 (dark green).

ferences in protein expression levels across different organ proteomes, where highly abundant contractile proteins such as myosin dramatically increases the dynamic range of the expressed muscle proteome (34) This high-quality dataset representing 213,000 unique peptides covering 12,909 protein-coding genes should represent a resource for the proteomics community, which can be bioinformatically mined or used as a general rodent spectral library for future DIA experiments.

Quantitative Rat Organ Protein Atlas by TMT and DIA-LFQ—We have previously demonstrated that it is possible to baseline resolve the isobaric TMT11-plex report ions in HCD scans recorded with 15,000 resolution and processed with phase-constrained spectrum deconvolution (phi-SDM), which resulted in >50% more identifications with >99% quantified proteins compared with standard settings (22). This phi-SDM method is implemented as a standard scan option termed Turbo-TMT in the methods editor for the Orbitrap Exploris 480 MS. Consequently, all TMT experiments were recorded with Turbo-TMT to maximize proteome coverage. To fit the 12 organs into a single TMT11-plex experiment, we pooled the duodenum, jejunum and ileum samples into one combined small intestine sample. Likewise, to increase reproducibility in peptide sequencing and enhance quantitative precision by facilitating normalization across the replicate batches, we included a common reference sample created by mixing aliquots of all tissues, in each of the three TMT11-plex batches covering the 10 organs from the three animals (supplemental Fig. S4*A*). To maximize proteome coverage in the TMT experiments, we performed offline HpH chromatography and collected 46 fractions, which we analyzed by online DDA-based LC-MS/MS using the turbo-TMT method. In contrast, for label-free quantitation we performed single-shot DIA-FAIMS experiments using the individual organ-specific spectral libraries for identification matching in Spectronaut. Consequently, the DIA experiments of the 12 organs analyzed in biological triplicates were performed in just 14 h of LC-MS/MS analysis time (except the time needed for generating the spectral library), whereas the three TMT11-plex batches

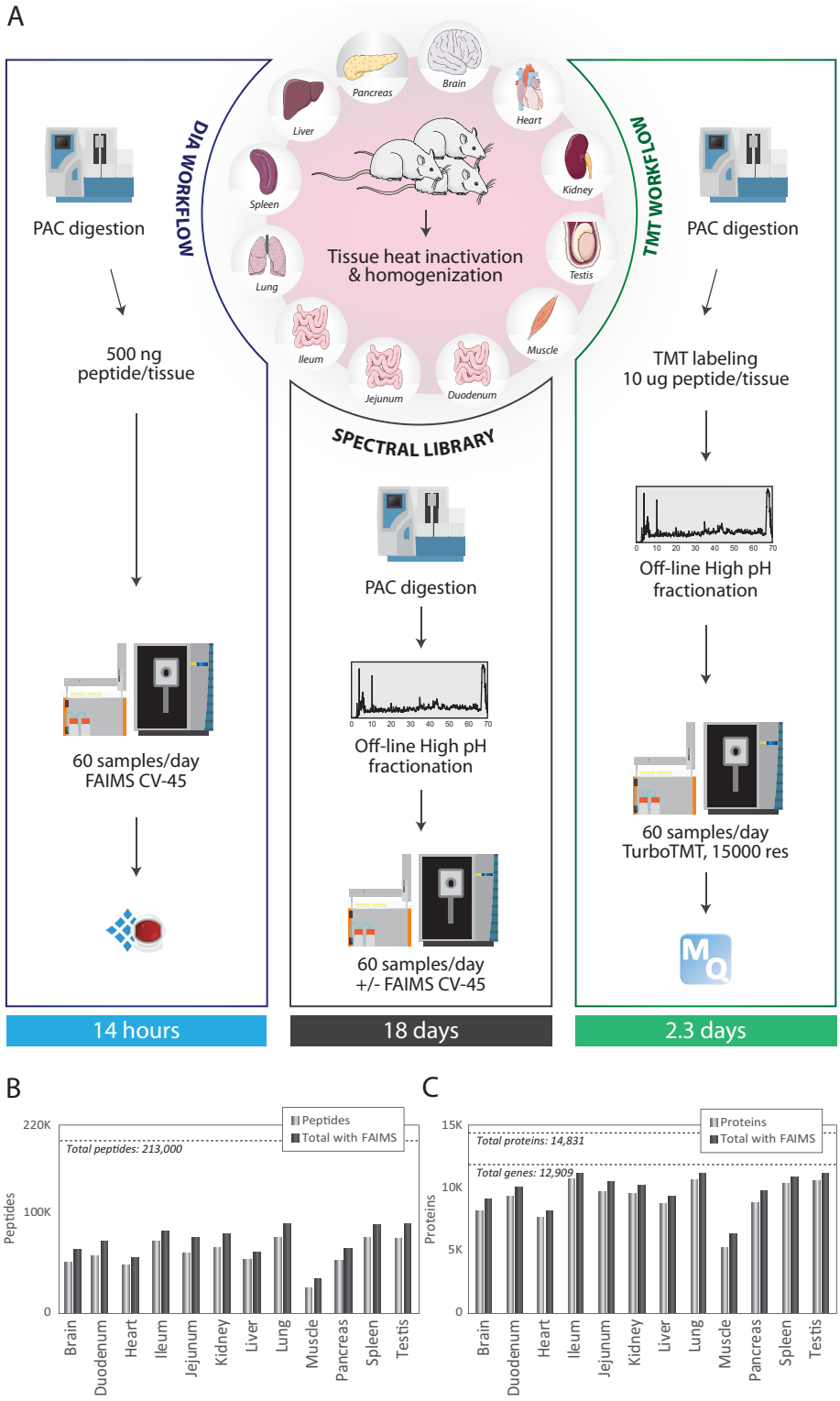

FIG. 4. ***A,* Experimental workflow of the rat tissue atlas.** *B*, Bar chart showing the number of peptides quantified in each single tissue library (light gray bar) and the gain in peptides after merging two libraries for the same tissue, one acquired without FAIMS and one acquired with FAIMS at CV-45 (dark gray). Dashed line indicates the total number of peptides identified in the complete library generated from the 12 tissues acquired with and without FAIMS. *C*, Bar chart showing the number of protein groups quantified in each single tissue library (light gray bar) and the gain in peptides after merging two libraries for the same tissue, one acquired without FAIMS and one acquired with FAIMS at CV-45 (dark gray). Dashed lines indicate the total number of protein groups and protein coding genes quantified in the complete library generated from the 12 tissues acquired with and without FAIMS.

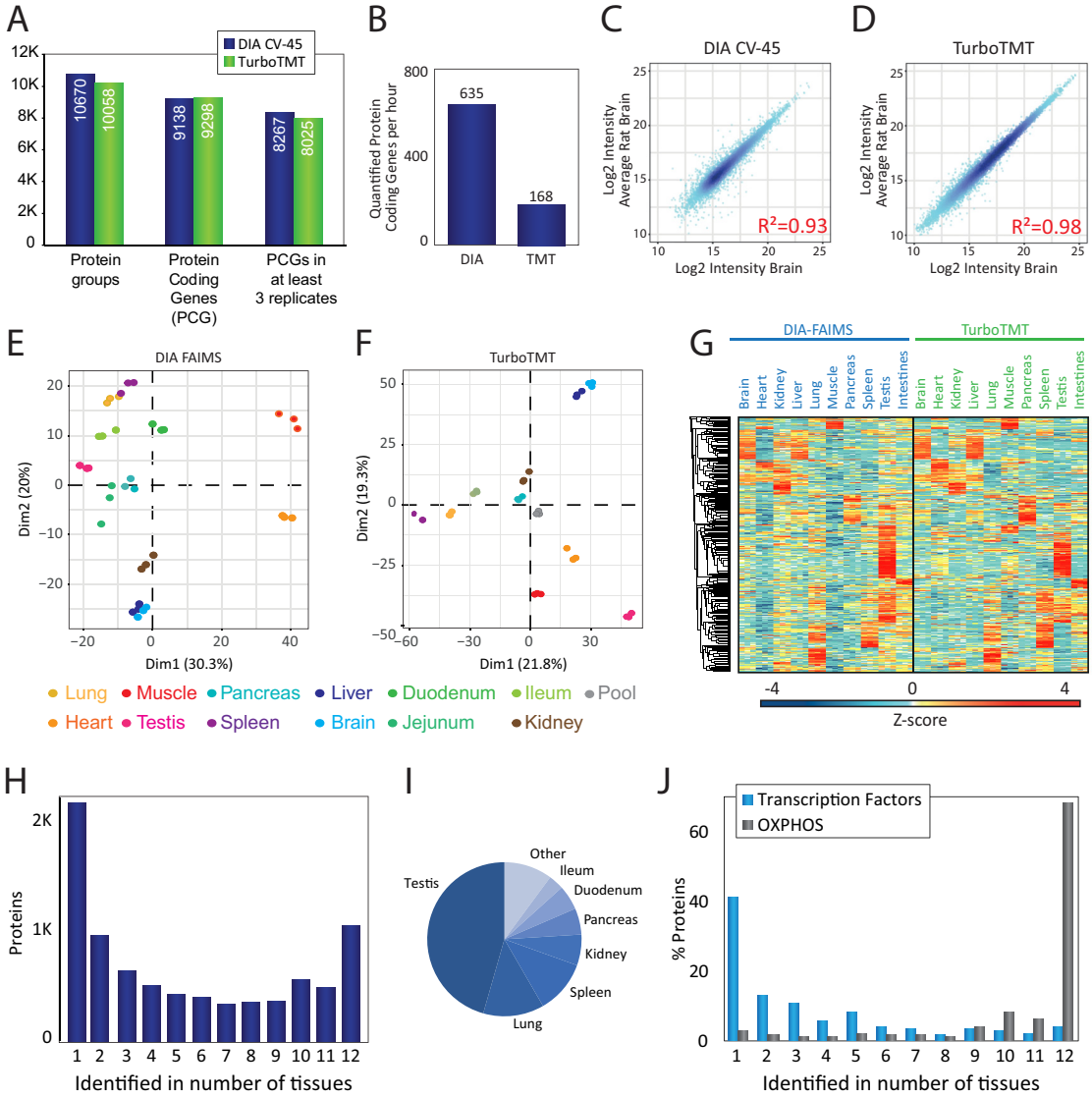

FIG. 5. ***A*, Bar chart showing the number of protein groups, protein coding genes (PCGs) identified and PCGs quantified in three replicates of the same tissue using DIA and FAIMS (dark blue) or turboTMT (green).** *B*, Number of PCGs per hour quantified in the DIA-FAIMS and turboTMT experiments. *C*, Correlation plot of the log2 intensity of each protein quantified in each rat brain against the average of the other two replicates from the same tissue in DIA-FAIMS. Correlation is measured as R-squared. *D*, Correlation plot of the log2 intensity of each protein quantified in each rat brain against the average of the other two replicates from the same tissue in turbo-TMT. Correlation is measured as R-squared. *E*, Principal Component Analysis (PCA) showing the classification of the 12 tissues from the three rats analyzed in the DIA-FAIMS experiment. *F*, Principal Component Analysis (PCA) showing the classification of the 10 tissues and the pooled sample from the three rats analyzed in the turbo-TMT experiment. *G*, Hierarchical clustering of the intensity (plotted as z-score) of the proteins identified in DIA-FAIMS and turbo-TMT experiments. *H*, Bar chart describing the number of specific proteins identified across tissues, where 1 indicates that the protein has only been identified in three replicates of the same tissue and 12 indicates that it has been quantified in all tissues. *I*, Pie chart showing the tissue-specificity of proteins identified in only one tissue. *J*, Bar chart depicting the percentage of proteins, either transcription factors (blue) or enzymes from the Oxidative Phosphorylation pathway (gray), expressed in different number of tissues.

required ~2.3 days of total mass spectrometric analysis time (Fig. 4*A*). Both quantification strategies resulted in comparable proteome coverage with more than ten thousand proteins quantified in total. More than eight thousand protein-coding genes were reproducibly quantified in all three TMT experiments, where each TMT set corresponds to one single rat (supplemental Table S4). In contrast, DIA-FAIMS highlights the tissue specificity of the proteomes with variable number of protein groups identified per tissue, from more than 5000 proteins in testis to 2000 proteins on average in muscle (supplemental Fig. S4*B*). Importantly, merging the protein coding genes quantified in each tissue in all three rats resulted in more than 8,000 proteins (Fig. 5*A* and supplemental Table S5), achieving a similar coverage as in TMT. This yields iden-

tification rates of more than 600 proteins per minute for DIA (Fig. 5*B*). To remove the batch bias between TMT experiments, we used ComBat normalization (29) and compared the normalized protein abundance reproducibility between the biological replica experiments for both TMT and DIA. We generally observed high reproducibility analyzing correlations of the log2-transformed protein intensities with R-squared of $r^2 = 0.93$ for DIA (Fig. 5*C*) and $r^2 = 0.98$ for TMT (Fig. 5*D*). The higher correlation for TMT experiments likely reflects the greater number of peptides identified per protein on average (35). To compare the reproducibility of the three biological replicates of all the rat organ proteomes analyzed by TMT and DIA, respectively, we performed a principal component analysis (PCA) of the normalized protein intensity data for all tissues. Both TMT and DIA data show excellent reproducibility with replica always closer in PCA space than distances to other tissues (Fig. 5*E* and Fig. 5*F*). The first component in the DIA based quantification explains more of the variance than for the TMT data - mainly separating the myocyte-rich tissues, cardiac and skeletal muscle, from the other tissues, most likely because of their higher dynamic range of protein abundances. Unsupervised hierarchical clustering of relative protein abundances across tissues reveal very similar protein expression patterns between DIA-FAIMS and TMT experiments, suggesting that both quantification strategies provides very similar biological insights (Fig. 5*G*). An advantage of DIA-FAIMS in the employed experimental design is that it allows us to evaluate the tissue-specificity of the rat proteome. Therefore, we analyzed the distribution of proteins across all tissues to differentiate tissue-specific *versus* globally expressed proteins. A larger proportion of the identified proteins are tissue specific than commonly expressed with more than two thousand of the identified proteins exclusively found in one tissue and only about one thousand proteins found in all tissues (Fig. 5*H*). By far most tissue-specific proteins were found in testis (Fig. 5*I*), which is in line with observations made in other datasets of global tissue expression profiling (36). To investigate the biological roles of the tissue-specific *versus* the globally expressed proteins, we performed a gene ontology (GO) enrichment analysis across the protein-specific tissue distributions, and found that globally expressed proteins are enriched for mitochondrial proteins involved in oxidative phosphorylation, whereas transcription factors (37) are generally tissue-specific proteins (Fig. 5*J*). These findings are consistent with the fact that cellular housekeeping functions such as ATP production by oxidative phosphorylation is generic to all cell types, whereas tissue specificity is facilitated by temporal and spatial gene expression patterns, which are driven by transcription factors (38).

Rapid, Sensitive and Deep Phosphoproteomics—The abundance of a protein is not always a direct measure of its cellular activity, which is often modulated by dynamic post-translational modifications (PTMs) (39). Site-specific protein phosphorylation is one of the most important PTMs regulating essentially all cellular protein signaling networks by controlling protein activity, subcellular localization, turnover and especially protein-protein interactions (40). We have previously demonstrated that it is possible to reproducibly identify close to five thousand unique phosphopeptides from 200 μg TiO2-enriched HeLa in-solution digest in just 15 min of LC-MS/MS analysis on an Easy nLC1200 coupled to a Q Exactive HF-X instrument (7). This is equivalent to an analysis throughput of 45 samples per day. We have now streamlined and automated the entire phosphoproteomics workflow on the KingFisher Flex robot incorporating on-bead PAC digestion and magnetic Ti-IMAC phosphopeptide-enrichment, which enable parallel preparation of up to 96 phosphopeptide samples (23) (supplemental Fig. S5). Analyzing the phosphopeptides prepared from 200 μg HeLa using data-dependent acquisition with the 28 Hz HCD method on the Orbitrap Exploris 480 MS with the Evosep One using the 60 samples per day method resulted in identification of more than eight thousand unique phosphopeptides of which more than five thousand could be localized confidently (41) to a single amino acid (Fig. 6*A*). Consequently, the optimization of all steps in the entire workflow increases the coverage of the same HeLa phosphoproteome by more than fifty percent in shorter analysis time. To test if this automated phosphoproteomics workflow is also suitable for tissue samples, we analyzed the phosphoproteomes of the 12 organ tissues from the three individual rats. We recently demonstrated that a spectral library-free DIA search, directDIA, of phosphopeptide enriched samples is superior to DDA (28). We therefore applied this acquisition strategy to analyze the 36 samples, which only required 14 h of MS instrument time, and resulted in the identification of more than 22,000 unique peptide variants and more than 13,000 localized phosphosites (Fig. 6*B* and supplemental Table S6). Unsupervised hierarchical clustering of z-scored and log-transformed phosphorylation site intensities revealed high correlation between replica of the same tissue and tissue-specific phosphorylation patterns (Fig. 6*C*). To identify protein kinases that exhibit tissue-enhanced activity, we mapped all known kinase-substrates from PhosphoSitePlus (42) onto our dataset and calculated the fraction of known substrates identified in our dataset for each kinase in 1 to 12 tissues. This analysis revealed that CAMK2A is the most tissue-specific kinase with one-third of the identified substrates unique to a single tissue (Fig. 6*D*). Cluster analysis highlighted heart tissue as the organ with the highest CAMK2A activity, where it phosphorylates proteins involved in cardiac muscle contraction (43) (Fig. 6*E*). Conversely, the known substrates of cAMP-dependent protein kinase (PKACA) were more uniformly distributed across the tissues (Fig. 6*F*–6*G*). The fast and sensitive organ phosphoproteomics profiling presented here demonstrated that there are major differences in the phosphorylation patterns across

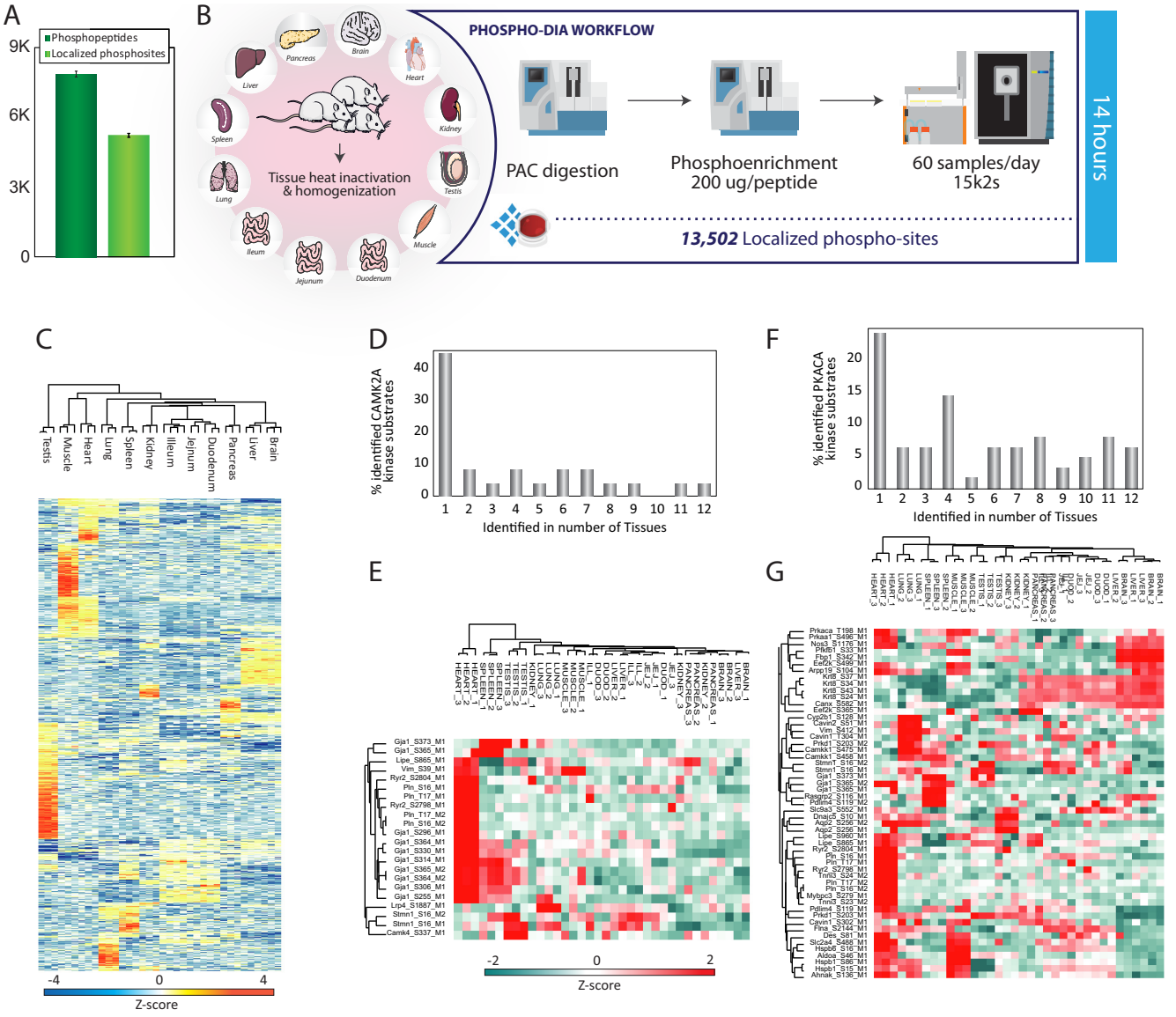

FIG. 6. ***A*, Number of phosphopeptides (dark green) and localized phosphosites (light green) from 200 μg of peptides enriched using Ti-IMAC-HP and analyzed with 21 min gradient.** *B*, Phospho-DIA workflow of 12 rat tissues from 3 independent rats *C*, Heatmap of ANOVA regulated phosphorylation sites of the rat tissues depicted as z-score. *D*, Bar plot showing the percentage of known CAMK2A substrates regulated in different number of tissues. *E*, Heatmap showing the differential regulation of phosphorylation in CAMK2A substrates across all rat tissues analyzed. *F*, Bar plot showing the percentage of known PKACA substrates regulated in different number of tissues. *G*, Heatmap showing the differential regulation of phosphorylation in PKACA substrates across all rat tissues analyzed.

tissues, and accordingly it can provide molecular insights into which and how signaling pathways are regulated in a tissue-specific manner.

CONCLUSION

The Orbitrap Exploris 480 MS is a compact hybrid quadrupole-Orbitrap mass spectrometer that provides high-quality HCD tandem mass spectra at acquisition rates of up to 40 Hz, which in combination with the Evosep One system, enables routine identification of more than 1,000 unique peptides per LC gradient minute. The application of FAIMS with a single CV increased proteome coverage in short gradients by close to 50% in data-dependent acquisition-based shotgun proteomics experiments of human cells at the expense of lower peptide coverage. Importantly, FAIMS enables analysis of minute sample amounts by effectively removing interfering singly-charged background ions. We demonstrate that it is possible to quantify more than 1,000 proteins from less than 50 HeLa cells with DIA-FAIMS, highlighting its potential for applications such as laser microdissected clinical samples and single-cell proteome analysis. The fast sequencing speed, high-sensitivity and robustness of the Orbitrap Exploris 480 MS makes it ideally suited for data-independent acquisition. The combination of FAIMS and data-independent acquisition pro-

vides more peptides identified and up to 5,100 mammalian proteins quantified in single-shot analysis using short LC gradients, allowing up to 60 samples to be measured in 24 h. This acquisition strategy enables high-throughput and large-scale profiling of hundreds of samples, as demonstrated by the quantitative organ tissue atlas we provide here, which includes a high-quality spectral library consisting of more than two hundred thousand unique peptides covering 12,900 protein-coding genes. This dataset comprises, to our knowledge, the deepest rat proteome to date. This spectral library was recorded by analyzing more than 1,000 LC-MS/MS runs of offline high pH reversed-phase peptide fractions back-to-back, which also demonstrates the robustness of the system throughout large-scale applications. In addition to label-free quantification the Orbitrap Exploris 480 MS is also optimized for tandem mass tag-based quantification enabled by the fast scanning turboTMT method. Additionally, we have presented a comprehensive benchmark of DIA-FAIMS against the well-established TMT-based quantification, showing that DIA-FAIMS provides equivalent proteome coverage as isobaric labeling. Interestingly, the observed biological reproducibility in TMT-based quantification was higher than for DIA-FAIMS, which likely reflects that all tissues from the same animal were combined in one TMT set. The limitation of analyzing 11 samples within a single TMT experiment is now ameliorated with the newly available TMT 16-plex reagents. Finally, the instrument is also a good match for quantitative analysis of post-translational modifications. Sensitive and large-scale analysis of cell line and organ phospho-proteomes is feasible in less than 1 day of analysis. Consequently, we envision that it will be find widespread use in many proteomics laboratories.

Acknowledgments—We thank our colleagues at Thermo Fisher Scientific, especially Jan-Peter Hauschild, Amelia Peterson, Erik Couzijn, Eduard Denisov, Denis Chernyshev, Christian Hock, Hamish Stewart, Ralf Hartmer, Christian Thoeing, Oliver Lange, Mathias Mueller, Arne Kreutzmann, Wilko Balschun, Aivaras Venckus, Alexander Kholomeev, Gregor Quiring, Frank Czemper, Andreas Wieghaus, Michael Belford, Julia Kraegenbring, Alexander Harder, Kerstin Strupat, Markus Kellmann. We would like to thank Stoyan Stoychev and Justin Jordaan for great help and input for optimizing our phospho-enrichment workflow and establishing automated platform for sample preparation. We would also like to thank Nicolai Bache for help and input on the chromatographic methods as well as Anna Secher for providing rat tissues and all members of the Olsen Group for critical input on the manuscript.

DATA AVAILABILITY

The mass spectrometry proteomics data have been deposited to the ProteomeXchange Consortium via the PRIDE partner repository. Data are available via ProteomeXchange with identifier PXD016662.

* Part of this work has been funded as part of the MSmed project that has received funding from the European Union's Horizon 2020 Research and Innovation program under grant agreement no. 686547 and as part of EPIC-XS project under the grant agreement no. 823839. Work at The Novo Nordisk Foundation Center for Protein Research (CPR) is funded in part by a generous donation from the Novo Nordisk Foundation (NNF14CC0001). J.V.O. and P.L.R. are supported by the Marie Skłodowska Curie European Training Network "TEMPERA" (grant number 722606). The authors declare the following competing financial interest(s): K.L.F., T.N.A., A.H., and A.A.M. are employees of Thermo Fisher Scientific, the manufacturer of the Orbitrap Exploris 480 MS instrument used in this research. The authors have declared a conflict of interest.

This article contains supplemental material.

** Current address: Evosep Biosystems, Odense, Denmark; E-mail: jesper.olsen@cpr.ku.dk.

¶ To whom correspondence should be addressed. Tel.: +45-353-25022; E-mail: jesper.olsen@cpr.ku.dk.

‖ These authors contributed equally to this work.

Author contributions: D.B.B.-J., A.M.-V., P.L.R., K.L.F., T.N.A., A.H., A.A.M., and J.V.O. designed research; D.B.B.-J., A.M.-V., S.S., P.L.R., K.L.F., T.N.A., A.H., A.A.M., and J.V.O. performed research; D.B.B.-J., A.M.-V., S.S., P.L.R., A.A.M., and J.V.O. analyzed data; D.B.B.-J., A.M.-V., P.L.R., A.A.M., and J.V.O. wrote the paper; K.L.F., T.N.A., A.H., and A.A.M. contributed new reagents/analytic tools.

REFERENCES

1. Kim, M. S., Pinto, S. M., Getnet, D., Nirujogi, R. S., Manda, S. S., Chaerkady, R., Madugundu, A. K., Kelkar, D. S., Isserlin, R., Jain, S., Thomas, J. K., Muthusamy, B., Leal-Rojas, P., Kumar, P., Sahasrabuddhe, N. A., Balakrishnan, L., Advani, J., George, B., Renuse, S., Selvan, L. D., Patil, A. H., Nanjappa, V., Radhakrishnan, A., Prasad, S., Subbannayya, T., Raju, R., Kumar, M., Sreenivasamurthy, S. K., Marimuthu, A., Sathe, G. J., Chavan, S., Datta, K. K., Subbannayya, Y., Sahu, A., Yelamanchi, S. D., Jayaram, S., Rajagopalan, P., Sharma, J., Murthy, K. R., Syed, N., Goel, R., Khan, A. A., Ahmad, S., Dey, G., Mudgal, K., Chatterjee, A., Huang, T. C., Zhong, J., Wu, X., Shaw, P. G., Freed, D., Zahari, M. S., Mukherjee, K. K., Shankar, S., Mahadevan, A., Lam, H., Mitchell, C. J., Shankar, S. K., Satishchandra, P., Schroeder, J. T., Sirdeshmukh, R., Maitra, A., Leach, S. D., Drake, C. G., Halushka, M. K., Prasad, T. S., Hruban, R. H., Kerr, C. L., Bader, G. D., Iacobuzio-Donahue, C. A., Gowda, H., and Pandey, A. (2014) A Draft Map of the human proteome. *Nature* **509,** 575–581
2. Wilhelm, M., Schlegl, J., Hahne H., Gholami, A. M., Lieberenz, M., Savitski, M. M., Ziegler, E., Butzmann, L., Gessulat, S., Marx H., Mathieson, T., Lemeer, S., Schnatbaum, K., Reimer, U., Wenschuh, H., Mollenhauer, M., Slotta-Huspenina, J., Boese, J. H., Bantscheff, M., Gerstmair, A., Faerber, F., and Kuster, B. (2014) Mass-spectrometry-based draft of the human proteome. *Nature* **509,** 582–587
3. Bekker-Jensen, D. B., Kelstrup, C. D., Batth, T. S., Larsen, S. C., Haldrup, C., Bramsen, J. B., Sørensen, K. D., Høyer, S., Ørntoft, T. F.; Andersen, C. L., et al. (2017) An optimized shotgun strategy for the rapid generation of comprehensive human proteomes. *Cell Syst.* **4,** 587–599
4. Makarov, A. (2019) Orbitrap journey: taming the ion rings. *Nat. Commun.* **10,** 3743
5. Kelstrup, C. D., Young, C., Lavallee, R., Nielsen, M. L., Olsen, J. V. (2012) Optimized fast and sensitive acquisition methods for shotgun proteomics on a quadrupole orbitrap mass spectrometer. *J. Proteome Res.* **11,** 3487–3497
6. Kelstrup, C. D., Jersie-Christensen, R. R., Batth, T. S., Arrey, T. N., Kuehn, A., Kellmann, M., Olsen, J. V. (2014) Rapid and deep proteomes by faster sequencing on a benchtop quadrupole ultra-high-field orbitrap mass spectrometer. *J. Proteome Res.* **13,** 6187–6195
7. Kelstrup, C. D., Bekker-Jensen, D. B., Arrey, T. N., Hogrebe, A., Harder, A., Olsen, J. V. (2018) Performance Evaluation of the Q Exactive HF-X for Shotgun Proteomics. *J. Proteome Res.* **17,** 727–738
8. Olsen, J. V, Macek, B., Lange, O., Makarov, A., Horning, S., Mann, M. (2007) Higher-energy C-trap dissociation for peptide modification analysis. *Nat. Methods* **4,** 709–712
9. Barnett, D. A., Ells, B., Guevremont, R., Purves, R. W. (2002) Application of ESI-FAIMS-MS to the analysis of tryptic peptides. *J. Am. Soc. Mass Spectrom.* **13,** 1282–1291
10. Saba, J., Bonneil, E., Pomie's, C., Eng, K., Thibault, P. (2009) Enhanced sensitivity in proteomics experiments using FAIMS coupled with a hybrid

linear ion trap/orbitrap mass spectrometer. *J. Proteome Res.* **8,** 3355–3366
11. Hebert, A. S., Prasad, S., Belford, M. W., Bailey, D. J., McAlister, G. C., Abbatiello, S. E., Huguet, R., Wouters, E. R., Dunyach, J. J., Brademan, D. R., et al. (2018) Comprehensive single-shot proteomics with FAIMS on a hybrid orbitrap mass spectrometer. *Anal. Chem.* **90,** 9529–9537
12. Schweppe, D. K., Prasad, S., Belford, M. W., Navarrete-Perea, J., Bailey, D. J., Huguet, R., Jedrychowski, M. P., Rad, R., McAlister, G., Abbatiello, S. E., et al. (2019) Characterization and optimization of multiplexed quantitative analyses using high-field asymmetric-waveform ion mobility mass spectrometry. *Anal. Chem.* **91,** 4010–4016
13. Pfammatter, S., Bonneil, E., McManus, F. P., Prasad, S., Bailey, D. J., Belford, M., Dunyach, J.-J., Thibault, P. (2018) A novel differential ion mobility device expands the depth of proteome coverage and the sensitivity of multiplex proteomic measurements. *Mol. Cell. Proteomics* **17,** 2051–2067
14. Pfammatter, S., Bonneil, E., Thibault, P. (2016) Improvement of quantitative measurements in multiplex proteomics using high-field asymmetric waveform spectrometry. *J. Proteome Res.* **15,** 4653–4665
15. Martins, C. P. B., Bromirski, M., Prieto Conaway, M. C., and Makarov, A. (2016) Orbitrap mass spectrometry: evolution and applicability. In *Applications of Time-of-Flight and Orbitrap Mass Spectrometry in Environmental, Food, Doping, and Forensic Analysis* (Perez, S., Eichhorn, P., and Barcelo, D. E., Ed.) Volume 71, pp 3–18, Elsevier, Amsterdam, the Netherlands
16. Scheltema, R. A., Hauschild, J. P., Lange, O., Hornburg, D., Denisov, E., Damoc, E., Kuehn, A., Makarov, A., Mann, M. (2014) The Q Exactive HF, a Benchtop Mass Spectrometer with a Pre-Filter, High-Performance Quadrupole and an Ultra-High-Field Orbitrap Analyzer. *Mol. Cell. Proteomics* **13,** 3698–3708
17. Michalski, A., Damoc, E., Hauschild, J. P., Lange, O., Wieghaus, A., Makarov, A., Nagaraj, N., Cox, J., Mann, M., Horning, S. (2011) Mass spectrometry-based proteomics using Q exactive, a high-performance benchtop quadrupole orbitrap mass spectrometer. *Mol. Cell. Proteomics* **10,** 10.1074/mcp.M111.011015
18. Senko, M. W., Remes, P. M., Canterbury, J. D., Mathur, R., Song, Q., Eliuk, S. M., Mullen, C., Earley, L., Hardman, M., Blethrow, J. D., et al. (2013) Novel parallelized quadrupole/linear ion trap/orbitrap tribrid mass spectrometer improving proteome coverage and peptide identification rates. *Anal. Chem.* **85,** 11710–11714
19. Lange, O., Damoc, E., Wieghaus, A., Makarov, A. (2014) Enhanced fourier transform for orbitrap mass spectrometry. *Int. J. Mass Spectrom.* **369,** 16–22
20. Werner, T., Becher, I., Sweetman, G., Doce, C., Savitski, M. M., Bantscheff, M. (2012) High-resolution enabled TMT 8-plexing. *Anal. Chem.* **84,** 7188–7194
21. McAlister, G. C., Huttlin, E. L., Haas, W., Ting, L., Jedrychowski, M. P., Rogers, J. C., Kuhn, K., Pike, I., Grothe, R. A., Blethrow, J. D., et al. (2012) Increasing the multiplexing capacity of TMTs using reporter ion isotopologues with isobaric masses. *Anal. Chem.* **84,** 7469–7478
22. Kelstrup, C. D., Aizikov, K., Batth, T. S., Kreutzman, A., Grinfeld, D., Lange, O., Mourad, D., Makarov, A. A., Olsen, J. V. (2018) Limits for resolving isobaric tandem mass tag reporter ions using phase-constrained spectrum deconvolution. *J. Proteome Res.* **17,** 4008–4016
23. Tape, C. J., Worboys, J. D., Sinclair, J., Gourlay, R., Vogt, J., McMahon, K. M., Trost, M., Lauffenburger, D. A., Lamont, D. J., Jørgensen, C. (2014) Reproducible automated phosphopeptide enrichment using magnetic TiO2 and Ti-IMAC. *Anal. Chem.* **86,** 10296–10302
24. Leutert, M., Rodríguez-Mias, R. A., Fukuda, N. K., Villén, J. (2019) R2-P2 rapid-robotic phosphoproteomics enables multidimensional cell signaling studies. *Mol. Syst. Biol.* **15,** e9021
25. Cox, J., Mann, M. (2008) MaxQuant enables high peptide identification rates, individualized p.p.b.-range mass accuracies and proteome-wide protein quantification. *Nat. Biotechnol.* **26,** 1367–1372
26. Cox, J., Neuhauser, N., Michalski, A., Scheltema, R. A., Olsen, J. V, Mann, M. (2011) Andromeda: a peptide search engine integrated into the MaxQuant environment. *J. Proteome Res.* **10,** 1794–1805
27. Bruderer, R., Bernhardt, O. M., Gandhi, T., Xuan, Y., Sondermann, J., Schmidt, M., Gomez-Varela, D., Reiter, L. (2017) Optimization of experimental parameters in data-independent mass spectrometry significantly increases depth and reproducibility of results. *Mol. Cell. Proteomics* **16,** 2296–2309
28. Bekker-Jensen, D. B., Bernhardt, O. M., Hogrebe, A., Val, A. M. del; Verbeke, L., Gandhi, T., Kelstrup, C. D., Reiter, L., Olsen, J. V. (2020) Rapid and site-specific deep phosphoproteome profiling by data-independent acquisition without the need for spectral libraries. *Nat. Comun.* **11,** 787
29. Leek, J. T., Johnson, W. E., Parker, H. S., Jaffe, A. E., Storey, J. D. (2012) The Sva package for removing batch effects and other unwanted variation in high-throughput experiments. *Bioinformatics* **28,** 882–883
30. Batth, T. S., Tollenaere, M. A. X., Rüther, P., Gonzalez-Franquesa, A., Prabhakar, B. S., Bekker-Jensen, S., Deshmukh, A. S., Olsen, J. V. (2019) Protein aggregation capture on microparticles enables multipurpose proteomics sample preparation. *Mol. Cell. Proteomics* **18,** 1027–1035
31. Bache, N., Geyer, P. E., Bekker-Jensen, D. B., Hoerning, O., Falkenby, L., Treit, P. V., Doll, S., Paron, I., Müller, J. B., Meier, F., et al. (2018) A novel LC system embeds analytes in pre-formed gradients for rapid, ultra-robust proteomics. *Mol. Cell. Proteomics* **17,** 2284–2296
32. Bruderer, R., Bernhardt, O. M., Gandhi, T., Miladinović, S. M., Cheng, L. Y., Messner, S., Ehrenberger, T., Zanotelli, V., Butscheid, Y., Escher, C., et al. (2015) Extending the limits of quantitative proteome profiling with data-independent acquisition and application to acetaminophen-treated three-dimensional liver microtissues. *Mol. Cell. Proteomics* **14,** 1400–1410
33. Svensson, M., Borén, M., Sköld, K., Fäith, M., Sjögren, B., Andersson, M., Svenningsson, P., Andrén, P. E. (2009) Heat stabilization of the tissue proteome: a new technology for improved proteomics. *J. Proteome Res.* **8,** 974–981
34. Deshmukh, A. S. (2016) Proteomics of skeletal muscle: focus on insulin resistance and exercise biology. *Proteomes* **4,** pii: E6
35. Hogrebe, A., von Stechow, L., Bekker-Jensen, D. B., Weinert, B. T., Kelstrup, C. D., Olsen, J. V. (2018) Benchmarking common quantification strategies for large-scale phosphoproteomics. *Nat. Commun.* **9,** 1045
36. Fagerberg, L., Hallstrom, B. M., Oksvold, P., Kampf, C., Djureinovic, D., Odeberg, J., Habuka, M., Tahmasebpoor, S., Danielsson, A., Edlund, K., et al. (2014) Analysis of the human tissue-specific expression by genome-wide integration of transcriptomics and antibody-based proteomics. *Mol. Cell. Proteomics* **13,** 397–406
37. Lambert, S. A., Jolma, A., Campitelli, L. F., Das, P. K., Yin, Y., Albu, M., Chen, X., Taipale, J., Hughes, T. R., Weirauch, M. T. (2018)The human transcription factors. *Cell* **172,** 650–665
38. Zhou, Q., Liu, M., Xia, X., Gong, T., Feng, J., Liu, W., Liu, Y., Zhen, B., Wang, Y., Ding, C., et al. (2017) A mouse tissue transcription factor atlas. *Nat. Commun.* **8,** 15089
39. Aebersold, R., Mann, M. (2016) Mass-spectrometric exploration of proteome structure and function. *Nature* **537,** 347–355
40. Lundby, A., Franciosa, G., Emdal, K. B., Refsgaard, J. C., Gnosa, S. P., Bekker-Jensen, D. B., Secher, A., Maurya, S. R., Paul, I., Mendez, B. L., et al. (2019) Oncogenic mutations rewire signaling pathways by switching protein recruitment to phosphotyrosine sites. *Cell* **179,** 543–560
41. Olsen, J. V., Blagoev, B., Gnad, F., Macek, B., Kumar, C., Mortensen, P., Mann, M. (2006) Global, in vivo, and site-specific phosphorylation dynamics in signaling networks. *Cell* **127,** 635–648
42. Hornbeck, P. V., Zhang, B., Murray, B., Kornhauser, J. M., Latham, V., Skrzypek, E. (2015) PhosphoSitePlus, 2014: mutations, ptms and recalibrations. *Nucleic Acids Res.* **43,** D512–D520
43. Santalla, M., Valverde, C. A., Harnichar, E., Lacunza, E., Aguilar-Fuentes, J., Mattiazzi, A., Ferrero, P. (2014) Aging and CaMKII alter intracellular Ca2+ transients and heart rhythm in Drosophila Melanogaster. *PLoS ONE* **9,** e101871